Letter to the Editor

Solid pilocytic astrocytoma in cavum septum pellucidum: a description of two cases and an analysis of misdiagnosis

Ming Liu[1], Dejiong Li[1], Shiguang Li[1], Yikuan Li[2], Guoping Zhang[1], Xiaofeng Jia[1], Menglei Fan[3]

[1]Department of Radiology, The Second People's Hospital of Guiyang (Jinyang Hospital), Guiyang, China; [2]Nuffield Department of Women's and Reproductive Health, Medical Science Division, University of Oxford, Oxford, UK; [3]Department of Pathology, The Second People's Hospital of Guiyang (Jinyang Hospital), Guiyang, China

Correspondence to: Ming Liu, MD. Department of Radiology, The Second People's Hospital of Guiyang (Jinyang Hospital), 547 Jinyang South Road, Guanshanhu District, Guiyang 550081, China. Email: 120429414@qq.com.

Submitted Nov 16, 2023. Accepted for publication Apr 25, 2024. Published online May 24, 2024.
doi: 10.21037/qims-23-1625
View this article at: https://dx.doi.org/10.21037/qims-23-1625

Introduction

Pilocytic astrocytoma (PA), a benign tumor and a specific form of astrocytoma, originates from neuroglial precursor cells. It is a prevalent glial tumor in children, with an incidence of approximately 17.6% among children with primary tumors and 85% among those with cerebellar tumors. PA is more common in children aged 7 to 9 years and affects both males and females (1). It is typically found in specific areas of the brain, including the infratentorial cerebellar hemisphere, vermis, fourth ventricle, pons, hypothalamus, and dorsal thalamus, but is rare in the cerebral hemispheres and spinal cord (2,3) and has not been reported in the septum pellucidum. In this case report, we describe the magnetic resonance (MR) findings from two cases of PA located in the cavum septum pellucidum that was verified pathologically. Our goal is to outline the features of PA in the septum pellucidum while analyzing the causes of misdiagnosis. This information will serve as a guide for radiologists and neurosurgeons in conducting preoperative assessments.

Case presentation

All procedures performed in this study were in accordance with the ethical standards of the institutional and/or national research committee(s) and with the Declaration of Helsinki (as revised in 2013). Written informed consent was provided by the patient guardians for publication of this article and accompanying images. A copy of the written consent is available for review by the editorial office of this journal.

Case 1

A 15-year-old female complained of a headache for one month and vomiting for one day, which was accompanied by walking instability and nausea. She was referred to our hospital for cranial MR examination, and an intracranial mass was found. Routine blood, liver function, kidney function, blood lipid, tumor marker, and other laboratory results were unremarkable. Her family had no genetic history of disease.

Imaging findings

Axial computer tomography images (*Figure 1A*) showed a solid, slightly dense mass in the cavum septum pellucidum. Axial T1-weighted (*Figure 1B*) and axial T2-weighted imaging (*Figure 1C*) showed a predominantly isointense solid mass signal in the cavum septum pellucidum, which was an enlarged. Meanwhile, the susceptibility-weighted imaging (*Figure 1D*) showed scattered hemosiderin deposits in the lesion. The axial diffusion-weighted images (*Figure 1E,1F,*) showed no diffusion restriction of the lesion. Axial, coronal, and sagittal contrast-enhanced T1-weighted images (*Figure 1G-1I*) showed heterogeneous intense enhancement of the mass between the bilateral ventricles. Surgery confirmed that the tumor was located in the cavum septum pellucidum. The tumor was gray-red, soft, with clear borders and a

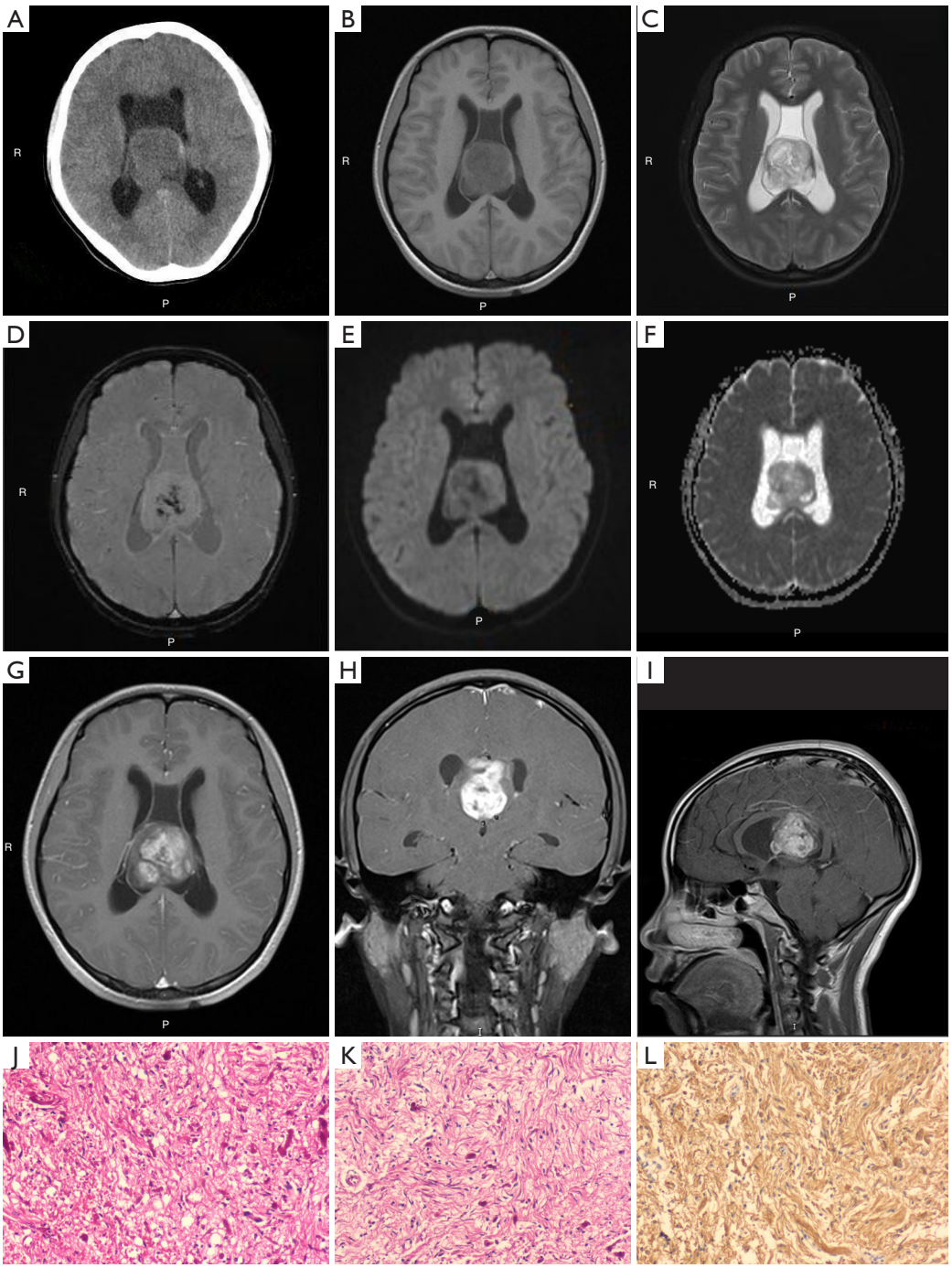

Figure 1 CT and MRI images and postoperative pathological sections of a 15-year-old female. (A) Axial cranial CT showed s a mass with slightly low density in the cavum septum pellucidum. (B,C) T1-weighted and T2-weighted axial views of MRI; the lesion in the cavum septum pellucidum displayed mixed signals with a predominantly iso-signal. (D) The susceptibility-weighted sequence of MRI showed scattered punctate hemorrhage within the lesion. (E,F) The DWI/ADC sequence showed the lesion without diffusion restriction. (G-I) Axial, coronal, and sagittal contrast-enhanced T1-weighted images showed intense enhancement of the lesion and enlargement of the lateral ventricle. (J,K) The pathological section (HE staining, 100×) of the mass showed bidirectional differentiation tissue features. (L) Histochemical GFAP staining was positive. Objective magnification 100×. CT, computed tomography; MRI, magnetic resonance imaging; DWI/ADC, diffusion-weighted images/apparent diffusion coefficient; HE, hematoxylin and eosin; GFAP, glial fibrillary acidic protein.

moderate blood supply. It was completely excised in a block under electrophysiological monitoring. Characteristics of bidirectional tumor differentiation, including dense area of spindle cells containing Rosenthal fibers and containing a sparse area of eosinophilic granular multipolar cells with microcyst formation, were found via hematoxylin and eosin staining (*Figure 1J,1K*). Glial fibrillary acidic protein (GFAP) staining was strongly positive in the dense area and weakly positive in the sparse area (*Figure 1L*). Other immunohistochemical results were as follows: GFAP+, S100+, Vimentin+, Olig-2+, ATRX foci+, SYN foci+, NF foci+, IDH-1–, CD34–. and Ki67 <1%+. PA [World Health Organization (WHO) grade 1] in the cavum septum pellucidum was confirmed with marked vascular proliferation in the focal area.

Case 2

A 12-year-old female complained of nausea and recurrent headache for three months with no obvious inducement, which was mainly located in the frontal and bilateral temporal areas. There were no positive findings in the physical examination and no special findings in blood routine, liver and kidney function, blood lipid, or infectious disease indices after admission.

Imaging findings

Axial T1-weighted (*Figure 2A*) and axial T2-weighted (*Figure 2B*) imaging showed a solid mass in the cavum septum pellucidum with an enlarged septal lumen. Axial diffusion-weighted/apparent diffusion coefficient imaging (DWI/ADC) (*Figure 2C,2D*) and susceptibility-weighted imaging (*Figure 2E*) revealed no diffusion restriction and scattered hemosiderin deposits in the lesion. Axial, coronal, and sagittal enhancement T1-weighted (*Figure 2F-2H*) imaging show heterogeneous intense enhancement of the mass. The tumor was compressing the foramen of Monro and had obstructed the flow of cerebrospinal fluid, which caused the lateral ventricle to expand. Axial fluid-attenuated inversion recovery (FLAIR) (*Figure 2I*) imaging showed heterogeneous hyperintensity of the mass. The tumor was resected in blocks under electrophysiological monitoring. The pathological sections of case 2 (*Figure 2J-2L*) demonstrated classic histopathologic features of PA that were similar to case 1 (*Figure 1J-1L*). The immunohistochemical components were almost the same in both cases.

Discussion

In the 2021 update of the WHO Classification of Tumors of the Central Nervous System (WHO CNS5), PAs are categorized as restricted astrocytomas with a WHO grade of 1 (4). The pathological features of PA consist of well-differentiated tumor cells with distinct regions of Rosenthal fiber bipolar cells and eosinophilic granular multipolar cells distributed in a bidirectional pattern. The tumor also exhibits intercellular glomerular vessels, thick-walled transparent vessels with large pores in the walls, strong positive immunohistochemistry for GFAP, S100, and OLIG2, and weak positive staining for SYN and α-B-crystallin expression (5). The symptoms of a tumor differ significantly based on its location in the brain and its size. Symptoms may include migraines, convulsions, limb weakness, and slurred speech. All instances of tumors in cases described in this report were situated in the septum pellucidum and manifested as symptoms of intracranial hypertension.

The cavum septum pellucidum is considered a standard structure in the developing human brain, which usually closes within a few months after birth but isn't closed in about 15% of adults. It is bounded anteriorly by the genu of the corpus callosum, superiorly by the body of the corpus callosum, posteriorly by the anterior limb and pillars of the fornix, inferiorly by the anterior commissure and the rostrum of the corpus callosum, and laterally by the leaflets of the septum pellucidum. The inner wall of the septum is not lined with ventricular canal cells, and therefore, the septum is not part of the ventricular system. The septum pellucidum is considered to be a membrane composed of white matter fibers and a modest amount of neuronal tissue. Lee and Manzano reported that in embryology, the septum pellucidum is formed by separation from the inner telencephalon during fornix formation and should be classified as a cortical structure containing glial cells (6). This theory explains how the septum pellucidum can be the site of origin of glioma, and the pathological manifestations of the two cases in this study are consistent with the criteria of PA in glioma.

The tumors of the two cases were closely related to the septum pellucidum, with smooth margins and a small amount of internal hemorrhage. MR imaging showed a solid lesion with predominantly isointense signal, with intense enhancement on the enhanced scan and no diffusion restriction on DWIC imaging or the ADC. For diagnosis, the relevant literature should be consulted

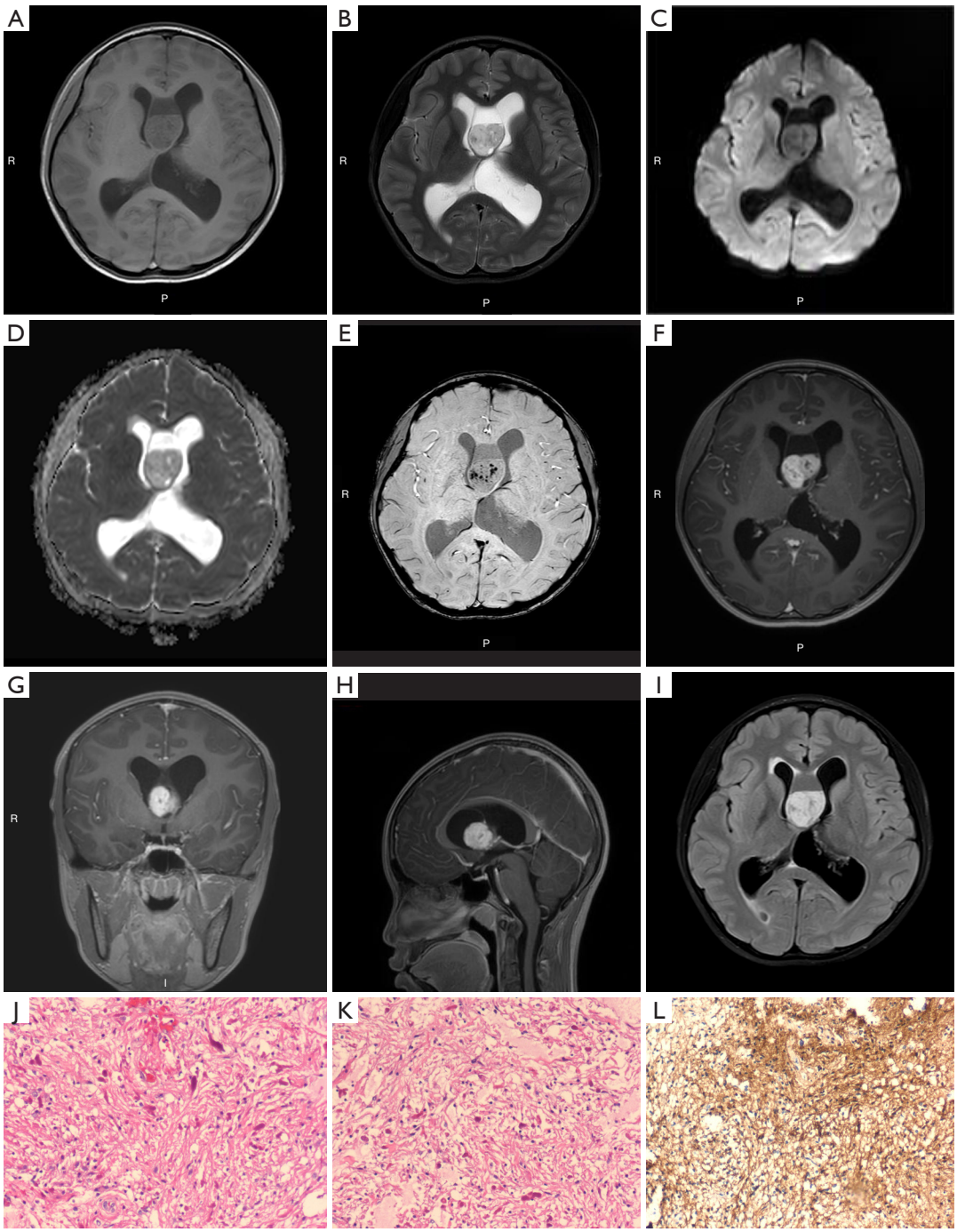

Figure 2 MRI images and postoperative pathological sections of a 12-year-old female. (A,B) Axial T1-weighted and axial T2-weighted MRI showed the lesion in the cavum septum pellucidum displaying mixed signals with predominant iso-signal. (C,D) The DWI/ADC sequence showed the lesion without diffusion restriction. (E) The susceptibility-weighted sequence showed scattered punctate hemorrhage within the lesion. (F-H) Axial, coronal, and sagittal contrast-enhanced T1-weighted images showed the mass with intense enhancement in the anterior part of an enlarged cavum septum pellucidum. (I) The axial FLAIR sequence showed heterogeneous hyperintensity of the mass. (J,K) Pathological section (HE staining, 100×) of the mass showed bidirectional differentiation tissue features. (L) Histochemical GFAP staining was positive. Objective magnification 100×. R, right; P, posterior; MRI, magnetic resonance imaging; FLAIR, fluid-attenuated inversion recovery; DWI/ADC, diffusion-weighted images/apparent diffusion coefficient; HE, hematoxylin and eosin; GFAP, glial fibrillary acidic protein.

according to the imaging features. The are several reports referring to glioblastoma in the septum pellucidum area (7,8). Glioblastoma is classified as a diffuse glioma species in adults in WHO CNS5, a malignant tumor of WHO grade 4 (1). Glioblastoma can easily lead to cystic transformation, necrosis, and hemorrhage, resulting in a poor prognosis. Typically, the onset occurs in middle and older age. In our cases, the imaging features did not match those of glioblastoma; therefore, this diagnosis was excluded preoperatively. Although there have been some reports of PA and chronic cystic hematoma with osseous metaplasia at the septum pellucidum, in our case, the diagnosis of PA and cystic hematoma was not made prior to surgery due to distinct imaging signs and lesion locations (9,10). There are other reports of glioneuronal tumor also growing in the septum pellucidum, such as dysembryoplastic neuroepithelial tumor (DNET) and myxoid glioneuronal tumor, which were excluded at the preoperative stage in both cases due to their mild enhancement being different from the features of PA (11,12). Napoli *et al.* reported that PA occurring in adulthood can mimic the MR imaging manifestations of high-grade tumors, especially because of its various shapes and susceptibility to cystic change, necrosis, and hemorrhage occurring in the ventricular system (13), which are obviously different from the location and manifestations of the cases reported here. Our cases were preoperatively misdiagnosed as central neurocytoma and germinoma based on the patient's age, the site of onset, and other related reports in the literature (14,15).

According to WHO CNS5, central neurocytoma (grade 2) belongs to the category of glial neuronal and neuronal tumors (4). It is a junctional low-grade malignant tumor, more prevalent in young people, and presumably of germ cell origin with bidirectional differentiation potential on the ventricular canal (16). The tumor is located in the anterior two-thirds of the lateral ventricle, near the foramen magnum, septum pellucidum, or lateral ventricle wall, and is densely packed with tumor cells. The lesions have a "fan-shaped" edge pattern, with cords connecting to the adjacent ventricular walls, and some of the lesions are surrounded by "vascular flow" signs. The diffusion of the solid part of the lesion is limited, with enhancement scans showing intense inhomogeneous enhancement (17). In a retrospective analysis of central neurocytoma, no DWI/ADC diffusion restriction was observed in the solid part of this tumor, and there were no typical "soap-bubble", "fan," "strip", or "vascular flow" signs. In our case, the tumor located in cavum septum pellucidum didn't exhibit typical features of a central neuroblastoma.

Germinoma tumors are classified as grade 4 germ cell tumors in the WHO CNS5 and are extremely aggressive (4). Germinoma is a highly malignant tumor that is usually found in adolescent, originates from intracranial residual germ cells, and can be multifocal and disseminated in the cerebrospinal fluid (18). Germinoma tumors in the basal ganglia, saddle area, corpus callosum, and pellucid septum have been reported in the literature, presumably due to the migration of ectopic germ cells from the midline during development (19). The MR findings of germinoma include a slightly high signal on T2, a slightly low signal on T1, and diffusion restriction on DWI, with hemorrhage and cystic lesions, no calcification, fuzzy borders, and theoretically no N-acetyl aspartate or creatine peaks in MR spectroscopy (20). In our cases, there was no elevation of the relevant tumor marker in the laboratory test and no multifocal distribution inside the brain, the lesion was well delineated, and the DWI/ADC was not diffusively limited, which did not precisely match the characteristics of a germinoma.

The factors contributing to why PA was not considered preoperatively can be summarized as follows: There was a lack of understanding regarding the origin and histology of the cavum septum pellucidum, leading to the oversight of the possibility of astrocytoma. Additionally, there was an insufficient interpretation of the imaging features of solid PA, as typical PA is mostly cystic solid, and the imaging features include a tumor within a capsule and a capsule within a tumor, while our cases showed a well-defined solid tumor with round shape, scattered hemorrhage, and no cystic changes. The diagnosis was hindered by the lack of cystic lesions and the presence of hemorrhage, and pathology of solid PA is characterized by numerous immature blood vessels causing internal hemorrhage, noticeable enhancement, oligocystic degeneration, and limited necrosis (21). Solid PA is primarily found in the hypothalamus, optic chiasm, and paraventricular thalamus, with no reported cases in the cavum septum pellucidum (22). Therefore, PA was not initially considered. It is believed that reporting these cases can expand the diagnostic consideration of radiologists and neurosurgeons as it relates to the diagnosis of tumors in the cavum septum pellucidum and provide an essential reference for research into the histology of the septum and PA oncology.

PAs seldom occurs in the telencephalons, and solid PAs are rare. Therefore, the solid PAs in the cavum septum

pellucidum reported in this paper will help readers increase their understanding of PA and expand their knowledge regarding the differential diagnosis of septum pellucidum masses.

Acknowledgments

Funding: None.

Footnote

Conflicts of Interest: Both authors have completed the ICMJE uniform disclosure form (available at https://qims.amegroups.com/article/view/10.21037/qims-23-1625/coif). The authors have no conflicts of interest to declare

Ethical Statement: The authors are accountable for all aspects of the work in ensuring that questions related to the accuracy or integrity of any part of the work are appropriately investigated and resolved. All procedures performed in this study were in accordance with the ethical standards of the institutional and/or national research committee(s) and with the Declaration of Helsinki (as revised in 2013). Written informed consent was provided by the patient guardians for publication of this article and accompanying images. A copy of the written consent is available for review by the editorial office of this journal.

References

1. Jacob K, Albrecht S, Sollier C, Faury D, Sader E, Montpetit A, Serre D, Hauser P, Garami M, Bognar L, Hanzely Z, Montes JL, Atkinson J, Farmer JP, Bouffet E, Hawkins C, Tabori U, Jabado N. Duplication of 7q34 is specific to juvenile pilocytic astrocytomas and a hallmark of cerebellar and optic pathway tumours. Br J Cancer 2009;101:722-33.
2. Chen J, Huang SL, Li T, Chen XL. In vivo research in astrocytoma cell proliferation with 1H-magnetic resonance spectroscopy: correlation with histopathology and immunohistochemistry. Neuroradiology 2006;48:312-8.
3. She DJ, Lu YP, Xiong J, Geng DY, Yin B. MR imaging features of spinal pilocytic astrocytoma. BMC Med Imaging 2019;19:5.
4. Louis DN, Perry A, Wesseling P, Brat DJ, Cree IA, Figarella-Branger D, Hawkins C, Ng HK, Pfister SM, Reifenberger G, Soffietti R, von Deimling A, Ellison DW. The 2021 WHO Classification of Tumors of the Central Nervous System: a summary. Neuro Oncol 2021;23:1231-51.
5. Schneider JF, Viola A, Confort-Gouny S, Ayunts K, Le Fur Y, Viout P, Bennathan M, Chapon F, Figarella-Branger D, Cozzone P, Girard N. Infratentorial pediatric brain tumors: the value of new imaging modalities. J Neuroradiol 2007;34:49-58.
6. Lee TT, Manzano GR. Third ventricular glioblastoma multiforme: case report. Neurosurg Rev 1997;20:291-4.
7. Takigawa K, Hata N, Sangatsuda Y, Suzuki SO, Sirozu N, Hatae R, Akagi Y, Iwaki T, Nagata S, Mizoguchi M. Intraventricular mucin-producing glioblastoma arising in the septum pellucidum at the frontal horn of the lateral ventricle: A case report. Neuropathology 2021;41:381-6.
8. Hariri OR, Quadri SA, Farr S, Gupta R, Bieber AJ, Dyurgerova A, Corsino C, Miulli D, Siddiqi J. Third Ventricular Glioblastoma Multiforme: Case Report and Literature Review. J Neurol Surg Rep 2015;76:e227-32.
9. Liu X, Dai X, Dai C, Zhu Q, Chen A, Chen Y, Chen N, Chen P, Rong R, Shi C, Xiao S, Dong J. Rare adult pilocytic astrocytoma of the septum pellucidum with novel RIN2::BRAF fusion. Virchows Arch 2023;482:445-50.
10. Roberti F, Bell J. Septum Pellucidum Chronic Encapsulated Hematoma With Osseous Metaplasia Mimicking Recurrent Astrocytoma and Shunt-Related Foreign Body Granuloma. Cureus 2020;12:e9839.
11. Solomon DA, Korshunov A, Sill M, Jones DTW, Kool M, Pfister SM, et al. Myxoid glioneuronal tumor of the septum pellucidum and lateral ventricle is defined by a recurrent PDGFRA p.K385 mutation and DNT-like methylation profile. Acta Neuropathol 2018;136:339-43.
12. Chiang JCH, Harreld JH, Tanaka R, Li X, Wen J, Zhang C, et al. Septal dysembryoplastic neuroepithelial tumor: a comprehensive clinical, imaging, histopathologic, and molecular analysis. Neuro Oncol 2019;21:800-8.
13. Di Napoli A, Spina P, Cianfoni A, Mazzucchelli L, Pravatà E. Magnetic resonance imaging of pilocytic astrocytomas

in adults with histopathologic correlation: a report of six consecutive cases. J Integr Neurosci 2021;20:1039-46.
14. Park DeWitt J, Kim YH, Han JH, Lee SH, Kim IH, Choe G, Kim CY. Primary intracranial germ cell tumor originating from septum pellucidum that mimics central neurocytoma. J Clin Oncol 2012;30:e274-7.
15. Boukobza M, Polivka M. Bifocal germinoma of the septum pellucidum and the sellar-supra-sellar region: An uncommon presentation for a rare tumor. eNeurologicalSci 2019;15:100187.
16. Ramsahye H, He H, Feng X, Li S, Xiong J. Central neurocytoma: radiological and clinico-pathological findings in 18 patients and one additional MRS case. J Neuroradiol 2013;40:101-11.
17. Donoho D, Zada G. Imaging of central neurocytomas. Neurosurg Clin N Am 2015;26:11-9.
18. Fang N, Wu Z, Wang X, Cao N, Lin Y, Li L, Chen Y, Cai S, Tu H, Kang D, Chen J. Rapid, label-free detection of intracranial germinoma using multiphoton microscopy. Neurophotonics 2019;6:035014.
19. Kim DI, Yoon PH, Ryu YH, Jeon P, Hwang GJ. MRI of germinomas arising from the basal ganglia and thalamus. Neuroradiology 1998;40:507-11.
20. Chang HY, Chiu CF, Jung SM, Wong AM, Wu CT, Lo FS. Neurological and endocrinological manifestations of 49 children with intracranial pure germinoma at initial diagnosis in Taiwan. Pediatr Neonatol 2021;62:106-12.
21. Parish JM, Bonnin JM, Payner TD, Goodman JM, Cohen-Gadol AA. Intrasellar pilocytic astrocytomas: clinical, imaging, pathological, and surgical findings. J Clin Neurosci 2015;22:653-8.
22. Foroughi M, Hendson G, Sargent MA, Steinbok P. Spontaneous regression of septum pellucidum/forniceal pilocytic astrocytomas--possible role of Cannabis inhalation. Childs Nerv Syst 2011;27:671-9.

Cite this article as: Liu M, Li D, Li S, Li Y, Zhang G, Jia X, Fan M. Solid pilocytic astrocytoma in cavum septum pellucidum: a description of two cases and an analysis of misdiagnosis. Quant Imaging Med Surg 2024;14(6):4269-4275. doi: 10.21037/qims-23-1625

